Redox proteomic profiling of neuroketal-adducted proteins in human brain: regional vulnerability at middle age increases in the elderly.

Mayelín Domínguez, Eliandre de Oliveira, María Antonia Odena, Manuel Portero, Reinald Pamplona, Isidro Ferrer

www.elsevier.com

PII: S0891-5849(16)00093-9
DOI: http://dx.doi.org/10.1016/j.freeradbiomed.2016.02.034
Reference: FRB12774

To appear in: *Free Radical Biology and Medicine*

Received date: 2 November 2015
Revised date: 3 February 2016
Accepted date: 27 February 2016

Cite this article as: Mayelín Domínguez, Eliandre de Oliveira, María Antonia Odena, Manuel Portero, Reinald Pamplona and Isidro Ferrer, Redox proteomic profiling of neuroketal-adducted proteins in human brain: regional vulnerability at middle age increases in the elderly., *Free Radical Biology and Medicine,* http://dx.doi.org/10.1016/j.freeradbiomed.2016.02.034

Redox proteomic profiling of neuroketal-adducted proteins in human brain: regional vulnerability at middle age increases in the elderly.

Mayelín Domínguez, MSc [a], Eliandre de Oliveira, PhD [b], María Antonia Odena, PhD [b], Manuel Portero MD, PhD [c], Reinald Pamplona MD, PhD [c], Isidro Ferrer, MD, PhD [a, d, e].*

[a] Institute of Neuropathology, University Hospital of Bellvitge, IDIBELL (Biomedical Research Institute of Bellvitge), Carrer Feixa Llarga sn, 08907, Hospitalet de Llobregat, Spain.
[b] Proteomics Platform, Barcelona Science Park, 08028, Barcelona, Spain.
[c] Department of Experimental Medicine, University of Lleida-Biomedical Research Institute of Lleida, 25198, Lleida, Spain.
[d] Department of Pathology and Experimental Therapeutics, University of Barcelona, Carrer Feixa Llarga sn, 08907, Hospitalet de Llobregat, Spain.
[e] CIBERNED (Centro de Investigación Biomédica en Red de Enfermedades Neurodegenerativas).

Author email addresses in order of appearance:
mdominguezg@idibell.cat, eoliveira@pcb.ub.es, maodena@pcb.ub.es, manuel.portero@mex.udl.cat, reinald.pamplona@mex.udl.cat, 8082ifa@gmail.com

**Corresponding author:,* Prof. Isidro Ferrer, Institut de Neuropatologia, Servei Anatomia Patologica, Hospital Universitari de Bellvitge, Carrer Feixa Llarga sn, 08907, Hospitalet de Llobregat, Spain., Phone number: +34 93 260 7452; Fax number: +34 93 260 7503, Email: 8082ifa@gmail.com

Abstract

Protein lipoxidation was assessed in the parietal cortex (PC), frontal cortex (FC), and cingulate gyrus (CG) in middle-aged and old-aged individuals with no clinical manifestations of cognitive impairment, in order to increase understanding of regional brain vulnerability to oxidative damage during aging. Twenty-five lipoxidized proteins were identified in all the three regions although with regional specificities, by using redox proteomics to detect target proteins of neuroketals (NKT) adduction. The number of cases with NKT-adducted proteins was higher in old-aged individuals but most oxidized proteins were already present in middle-aged individuals. Differences in vulnerability to oxidation were dependent on the sub-cellular localization, secondary structure, and external exposition of certain amino acids. Lipoxidized proteins included those involved in energy metabolism, cytoskeleton, proteostasis, neurotransmission and O_2/CO_2, and heme metabolism. Total NKT and soluble oligomer levels were estimated employing slot-blot, and these were compared between age groups. Oligomers increased with age in PC and FC; NKT significantly increased with age in FC, whereas total NKT and oligomer levels were not modified in CG, thus highlighting differences in brain regional vulnerability with age. Oligomers significantly correlated with NKT levels in the three cortical regions, suggesting that protein NKT adduction parallels soluble oligomer formation.

Key words:
aging, oxidative damage, oligomers, lipoxidation

Abbreviations

ACO2: aconitate hydratase; ATP5A1: ATP synthase subunit alpha; AD: Alzheimer's disease; BASP1: brain acid soluble protein 1; BLVRB: NADPH-flavin reductase; CA1: carbonic anhydrase 1; CG: cingulate gyrus; CKB: creatine kinase B-type; CRYAB: alpha-crystallin B chain; DHA: docosahexaenoic acid; DLD: dihydrolipoyl dehydrogenase; DPYSL2: dihydropyrimidinase-related protein 2; ENO1: alpha-enolase; FC: frontal cortex; GAPDH: glyceraldehyde-3-phosphate dehydrogenase; GFAP: glial fibrillary acidic protein; GO: gene ontology; GOT1: aspartate aminotransferase; HBA1: hemoglobin subunit alpha; HSPD1: 60 kDa heat shock protein; LC-MS/MS: liquid chromatography–tandem mass spectrometry; NEFL: neurofilament light polypeptide; NEFM: neurofilament medium polypeptide; NKT: neuroketals; PARK7: protein DJ-1; PC: parietal cortex; PEBP1: phosphatidylethanolamine-binding protein 1; PGAM1: phosphoglyceratemutase 1; PKM2: pyruvate kinase isozymes M1/M2 ; ROS: reactive oxygen species; SYN1: synapsin-1; TPPP: tubulin polymerization-promoting protein; UCHL1: ubiquitin carboxyl-terminal hydrolase L1; YWHAG: 14-3-3 protein gamma.

Introduction

Aging produces changes in the structure and function of biological systems, leading to increased vulnerability to disease and death [1]. Senescence results from the accruement of declining processes including unbalanced oxidation, accumulation of abnormal and damaging molecules, and loss of repair capacities, among other factors [2]. In the brain, aging is manifested by reduction in white matter size, selective loss of neurons, dendrites and dendritic spines, modifications in neurotransmission, and senescence of glial cells [3-6]. Regional vulnerability results from the vulnerability of a particular region to damage by distinct noxious stimuli together with its specific capacity to react to the harmful stimuli. The combination of external factors such as blood flow and internal factors such as specificities of distinct neuronal and glial cell types contributes to delineating regional brain profiles of vulnerability during aging [7].

Reactive oxygen species (ROS) have been implicated as sources of molecular injury when reaching undesirable thresholds [8-9] and have been directly implicated in the process of aging [10]. The human brain has high energy metabolism and high oxygen consumption demands, relatively low antioxidant defenses when compared with other tissues, high rates of transition metals that may act in redox cycles, and high concentration of poly-unsaturated fatty acids [11-12]. All these factors make the brain highly susceptible to oxidative stress damage during aging. Moreover, some targets of oxidative damage are common in aging and neurodegenerative diseases such as Alzheimer's disease (AD) [13-16].

Lipid peroxidation is an important source of secondary ROS-mediated injury. Poly-unsaturated fatty acids present in cell membranes are extremely susceptible to peroxidation [17]. Among these, docosahexaenoic acid (DHA; C22:6, ω3) is particularly abundant in the brain when compared to other ones such as arachidonic acid; DHA is highly concentrated in neuronal membranes and accounts for about one-third of total

fatty acids in amino-phospholipids of gray matter [18]. Neuroketals (NKT) are γ-ketoaldehyde sub-products of the non-enzymatic oxidation of DHA through the neuroprostane pathway [19]. NKT adducts lysine residues of proteins with remarkable rapidity causing protein lipoxidation and inducing cross-linking and aggregation [20], which are common marks of several age-related neurodegenerative disorders [21].

Soluble intermediates of protein aggregates named soluble oligomers cause cell injury by several mechanisms including mitochondrial damage, increased oxidative stress, and reduced protein clearance [22]. Soluble oligomers display a common conformation-dependent structure that is unique regardless of sequence and, therefore, allows detection with conformation-specific antibodies [23]. This suggests that they share a common mechanism of toxicity despite their derivation from different proteins [24]. A possible relation between oligomer production and NKT-mediated protein damage, and induction of cross-linking and aggregation, is a plausible hypothesis triggering cell damage.

Since the majority of the neurodegenerative diseases with abnormal protein aggregates appear in older individuals it is practical to try to gain understanding about modifications occurring with age before the time of the appearance of these diseases. The reason is not only to gain knowledge about mechanistic aspects but also to identify putative rational windows for specific therapeutic intervention. In the context of aging, redox proteomics is a very useful tool to identify protein targets of lipoxidative damage and to infer possible functional implications [25-26].

The present study analyzes lipoxidation in middle-aged and old-aged individuals with no clinical manifestations of cognitive impairment in three brain regions: parietal cortex, frontal cortex, and cingulate gyrus. Redox proteomics is used to detect target proteins modified by NKT adducts. This is followed by the bioinformatic analysis of factors contributing to vulnerability of NKT-adducted proteins, considering their localization, structure, and functions. Finally, the relation between the presence of soluble oligomeric species and NKT-adduction is explored in each region in the different age groups to learn about possible interactions of soluble oligomers and protein lipoxidation with age.

Methods

Samples

Brain tissue samples were obtained from eighteen cases from the Institute of Neuropathology Brain Bank, a branch of the HUB-ICO-IDIBELL Biobank, following the guidelines of the Spanish legislation and the approval of the local ethics committee. At autopsy, each brain was rapidly removed from the skull. The left hemisphere was fixed in 4% buffered formalin for neuropathological study and the right hemisphere cut into slices, dissected into selected regions which were separated in individual labeled plastic bags, immediately frozen, and stored at -80ºC until use. Three regions were studied: parietal cortex Brodmann area 7 (PC), frontal cortex area 8 (FC), and cingulated gyrus area 23 (CG).

A routine neuropathological study was performed in every case [27]. The neuropathological examination did not reveal lesions excepting moderate small blood vessel disease and status cribosus, and a few neurofibrillary tangles consistent with

AD-related pathology stage I of Braak and Braak in older cases. In no cases were diffuse and neuritic β-amyloid plaques present. Therefore, hallmarks of AD-related pathology were not observed in the PC, FC, and CG in any case.

The age of subjects ranged from 40 to 79 years (mean 58.9 ± 13.5 years) and five of them were females (27.8%). The mean post-mortem delay was 6h15min ± 2h48min (minimum 2h, maximum 14h). Markers of protein/nitrosative damage are preserved in post-mortem brains within these post-mortem time points [27]. All samples used were from individuals who did not have neurological or mental diseases, and had not suffered from diabetes, hepatic failure, or renal failure. In all of them there was an absence of prolonged hypoxia, sepsis, and agonal state in the context of artificial respiratory assistance. The causes of death in these cases were variable including carcinoma non-affecting the central nervous system, cardiac infarction, pulmonary thrombosis-embolism, and pneumonia. Summary of cases is shown in Table 1.

Two-dimensional (2D) gel electrophoresis

Samples of the PC, FC, and CG from ten individuals were analyzed with 2D electrophoresis (Table 1). These cases were representative of two age groups: five were middle-aged cases (mean age 43 ± 2.8 years) and five were old-aged cases (mean age 74 ± 5.5 years). The totality of samples was processed on different days. From each region, 0.1g of frozen tissue was homogenized in 1mL of ice-cold lysis buffer (7M Urea, 2M Thiourea, 40mM Tris pH 7.5 and 4% CHAPS) containing phosphatase and protease inhibitors (Roche Molecular Systems). The homogenate was centrifuged at 16,000g for 10min at 4°C and the pellet was discarded. Proteins from 300µL of the resulting supernatant were precipitated with methanol/chloroform at room temperature. Protein pellets were then suspended in 300µL of lysis buffer. Protein concentration was determined with the Bradford assay with bovine serum albumin (Sigma-Aldrich) as standard.

For the first dimension electrophoresis, equal amounts of protein (200µg) in lysis buffer from each sample were mixed with 0.8% Byo-Lyte 3/10 ampholyte, 5mM TBP, and 0.0004% bromophenol blue. Next, the sample was applied onto 7 cm pH 3-10 NL ReadyStrip™ IPG strips (Bio-Rad) for isoelectric focusing on a Protean® IEF Cell system (Bio-Rad) at 20°C and current limit of 50µA per strip. The strips were actively re-hydrated at 50V for 14h and focused in sequential steps of 1h at 200V, 1h at 500V, 1h at 1,000V, 1h at 8,000V, and 10h at 8,000V. After focusing, the strips were stored at -20°C until required.

For the second dimension, the strips were re-equilibrated in equilibration buffer (6M urea, 50mM Tris-HCl pH 8.8, 2% SDS, and 20% glycerol) containing 5mM TBP, and then alkylated in the same buffer plus 2.5% IAA. Afterwards, the strips were placed on the top of 10% SDS-polyacrylamide gels and electrophoresed at 120V at 4°C. Two identical gels were run in parallel for each sample. One was silver stained using the PlusOne™ Silver Staining Kit as described by the manufacturer (GE Healthcare). The other one was processed for western blotting.

NKT-adducted protein identification

The goat anti-NKT antibody (dilution 1:2,000, Ab5611, Chemicon International) was used to detect NKT-adducted proteins. According to the indications of the supplier, the antibody, produced using neuroketal-conjugate as immunogen, has been shown to react with neuroketal/neuroprostane-modified proteins by ELISA. By western blotting,

the antibody reacts with several major and many minor bands in human brain protein modifications.
This antibody has been previously used and validated in several brain regions and neurological diseases [28-30].
NKT-positive spots in the 2D gels were qualitatively compared by visual inspection between age groups. The selection of NKT-positive spots was based on the presence or increased intensity in old-aged individuals versus absence or reduced intensity in middle-aged individuals.
Selected NKT-adducted protein spots detected by western blot were matched with corresponding silver-stained spots in parallel gels. Selected spots were excised from 2D silver stained gels and subjected to in-gel tryptic digestion using the automatic protein digestion system Investigator™ Progest (Genomic Solutions). Briefly, the SDS-gel spots were cleaned with 25mM ammonium bicarbonate and acetonitrile. Next, the sample was reduced (10mM dithiothreitol for 30 min at 56°C) and alkylated (55mM iodoacetamide for 30min at 21°C in the dark). Afterwards, each sample was digested overnight at 37°C with 80ng of sequencing grade modified trypsin (Promega). Finally, the resulting peptide mixture was extracted from the gel matrix with 10% formic acid and acetonitrile, and then dried-down.
The dried-down peptide mixture was analyzed in a nanoAcquity liquid chromatographer (Waters) coupled to a LTQ-Orbitrap Velos (Thermo Scientific) mass spectrometer. Tryptic peptides were re-suspended in 1% formic acid and each aliquot was injected into a nanoAcquity Symmetry C18 trap column (5µm, 180µm x 20mm; Waters). Trapped peptides were separated using a C18 nanoAcquity reverse phase capillary column (75µm x 100mm, 1.7µm BEH130, Waters). The gradient used for elution of peptides was 0 to 40% B in 20 min, followed by a gradient from 40% to 60% in 5 min with a 250 nL/min flow rate (mobile phases, A and B, were composed of 0 and 100% acetonitrile, respectively, and each contained 0.1% formic acid). Eluted peptides were subjected to electrospray ionization in an emitter needle PicoTip™ (New Objective) with an applied voltage of 2,000V. Peptide masses (m/z 350-1700) were analyzed in data-dependent mode with a full Scan MS in the Orbitrap with a resolution of 60,000 FWHM at 400m/z. Up to 5 of the most abundant peptides (minimum intensity of 500 counts) were selected from each MS scan. Then, they were fragmented by collision induced dissociation in a linear ion trap using helium as collision gas with 38% normalized collision energy. Generated raw data were collected with Thermo Xcalibur v.2.1.0.1140 (Thermo Scientific).
Protein identification
Raw data were submitted for database searching with the Mascot search engine using Thermo Proteome Discover v.1.3.0.339 (Thermo Scientific) against Swiss-Prot database. Both target and a decoy database were searched to obtain a false discovery rate (FDR) and thus estimate the number of incorrect peptide-spectrum matches exceeding a given threshold. The following search parameters were applied: trypsin enzyme, 2 missed cleavages, carbamidomethyl of cysteine as fixed modification, oxidation of methionine as variable modification, and peptide tolerance of 10 ppm and 0.6Da (for MS and MS/MS spectra, respectively).
To improve the sensitivity of the database search, Percolator (semi-supervised learning machine) was used to discriminate correct from incorrect peptide spectrum matches. Percolator assigns a q-value to each spectrum, which is defined as the minimal FDR at which the identification is deemed correct. These q values are estimated using the

distribution of scores from decoy database search (Percolator Target FDR, strict: 0.01; Validation based on: q-value). The list of resulting proteins was filtered to accomplish two restrictions: containing *Homo sapiens* in the description and having at least 2 high-confidence peptides (FDR ≤ 0.01).

Western-blotting

2D gels obtained in a sub-set of samples were used to detect NKT-adducted proteins. Total number of cases (n=18) was analyzed by western blotting for total levels of selected proteins in mono-dimensional (1D) gels. Equal amounts of total protein for each sample were loaded onto 10% SDS-polyacrylamide gels and separated according to their molecular weight. Polyacrylamide gels (1D or 2D) were transferred onto nitrocellulose membranes using the Trans-Blot® Turbo™ blotting system (Bio-Rad). Transferred membranes were blocked with 5% skimmed milk in TBS-T buffer and incubated overnight at 4°C with the appropriate primary antibody diluted with 3% BSA in TBS-T. Then the membranes were washed in TBS-T and incubated with the corresponding secondary antibody labeled with horseradish peroxidase (HRP), and washed again in TBS-T. Immunoreactivity was detected with the chemiluminescence method (Amersham ECL Western blotting detection reagents, GE Healthcare).

To validate the LC-MS/MS identification results, selected proteins were tested with the corresponding antibodies on the same 2D membranes after stripping. Strip of membranes consisted of two sequential washes in stripping buffer (62.5mM Tris-HCl pH 6.8, 2% SDS, 100mM β-mercaptoethanol) at 65°C, three washes in TBS-T at room temperature, and blockage with 5% skimmed milk in TBS-T buffer. A list of the antibodies employed is shown in Supplementary Table 1.

Slot-blot

The level of soluble oligomeric species was detected with slot blot analysis using the anti-oligomers A11 antibody (AHB0052, Invitrogen) according to the manufacturer's protocol for dot-blotting. A11 antibody detects specific oligomeric structural conformations. Previous to this analysis, A11 antibody was tested (by slot-blot with the same protocol) against monomeric $A\beta_{40-42}$; no signal was detected thus confirming the specificity of the assay. In order to obtain soluble proteins at non-denaturing concentrations of compounds on the original lysis buffer, samples were diluted 1:10 (v/v) in phosphate buffered saline (137mM NaCl, 2.7mM KCl, 10mM Na_2HPO_4, 2mM KH_2PO_4 pH 7.4) and allowed proteins to re-nature minimizing aggregation. Then, samples were centrifuged at 16,000g for 5min at room temperature; the insoluble pellet was discarded and protein concentration determined by Bradford assay.

Equal amounts of total protein of each sample were slot-blotted onto nitrocellulose membranes by vacuum using a SHM-48 slot blotter unit (Scie-Plas). Ponceau staining (AppliChem GmbH) was used to verify equal protein loads after blotting. The membranes were blocked in 10% skimmed milk, incubated overnight with A11 antibody, washed, incubated with the secondary anti-rabbit HRP conjugated antibody, and washed using buffers and dilutions recommended by the supplier. Immunoreactivity detection was performed with chemiluminescence as for western-blots. After oligomer detection, the membranes were stripped and tested against NKT to explore possible quantitative relation in the amount of NKT and oligomeric species in the same protein fraction as well as total NKT levels.

Densitometry

Densitometry of monodimensional gel protein bands and slots was used to determine expression levels. The quantification analysis was performed with TotalLab software (Nonlinear Dynamics). β-tubulin in monodimensional gels and total protein (from Ponceau staining) in slots were used as internal controls of protein loading prior to statistical analysis.

Bioinformatics-based protein characterization

Proteins under study were identified by their UnitProt database accession numbers (http://www.uniprot.org/); particular cellular locations and functions are reported in accord with this database. For analysis of the structural features PredictProtein web-based software (https://www.predictprotein.org/) was employed. Functional protein-protein interaction network analysis was performed using the web-based STRING software (http://www.string-db.org/) [31]. Gene Ontology (GO) and pathway analysis was performed using Cytoscape software with the ClueGO and CluePedia plugins including information from KEEG, REACTOME, and STRING databases [32, 33].

Statistical analyses

Descriptive data were expressed as mean ± standard deviation or as percentages when needed. Kruskal-Wallis test with Lilliefors correction was used to probe the normality assumption for continuous variables. Student's *t* test and Mann-Whitney U test, as appropriate, were used to evaluate differences between age groups. Pearson correlations were employed to assess possible relations among variables. In addition, NKT and soluble oligomer levels were subjected to factor analysis using Principal Components Analysis (PCA). For all the tests, p-values less than 0.05 were considered statistically significant. Statistical analyses were carried out using STATISTICA v8.0 software (StatSoft).

Results

2D gel electrophoresis and NKT adducted-protein identification

PC, FC, and CG samples of the ten cases covering the two groups of age distribution (middle-aged, old-aged) were analyzed with 2D electrophoresis and anti-NKT western blotting. NKT-positive spots were qualitatively compared by visual inspection between age groups. Thirty-nine NKT-positive spots were selected as being of interest based on increased intensity or presence in old-aged individuals (Figure 1). The corresponding spots in the silver-stained gels processed in parallel were excised, in-gel digested, and analyzed with LC-MS/MS for protein identification. The full list of spots and the corresponding LC-MS/MS resulting identifiers is shown in Table 2.

Validation of identified proteins

In order to corroborate that protein gel spots were accurately identified by LC-MS/MS, thirteen top candidate proteins (ATP5A1, BASP1, CKB, CRYAB, ENO1, GAPDH, GFAP, HBA1, HSPD1, NEFL, PARK7, UCHL1 and YWHAG) were analyzed. 2D anti-NKT blotted membranes were stripped and blotted against specific antibodies corresponding to proteins of interest (Supplementary Figure 1). The resulting spots were matched with the original ones over the same 2D membrane, and protein

identities were corroborated. However, UCHL1 matched a group of NKT-positive spots but displaced to a more basic isoelectric point.

NKT adducted proteins with respect to age in each region

A final list of twenty-five protein targets of lipoxidation by NKT adduction is shown in Table 3 which includes their locations and functions. The number of cases per age group and region in which proteins were oxidized is presented in Figure 2.

In the PC (Figure 2A), 8 proteins (32%) showed the same levels of lipoxidation in both age groups (ATP5A1, DLD, GFAP, NEFL, NEFM, HSPD1, BASP1, and SYN1) while 17 (68%) manifested increased lipoxidation with age (CKB, GAPDH, PGAM1, ENO1, PKM2, ACO2, TPPP, PARK7, CRYAB, GOT1, DPYSL2, YWHAG, HBA1, CA1, BLVRB, PEBP1, and UCHL1). Four of them (PKM2, ACO2, CRYAB, and HBA1) were oxidized only in old-aged cases.

In the FC (Figure 2B), 6 proteins (24%) showed no differences in the presence of NKT adduction between middle-aged and old-aged individuals (CKB, GAPDH, GFAP, NEFL, NEFM, and HSPD1) whereas 19 proteins (76%) presented increase in the NKT adducted forms in old-aged individuals (PGAM1, ENO1, PKM2, ACO2, ATP5A1, DLD, TPPP, PARK7, CRYAB, GOT1, DPYSL2, BASP1, YWHAG, HBA1, CA1, BLVRB, PEBP1, SYN1, and UCHL1). One protein, HBA1, was lipoxidized only in old-aged individuals.

In the CG (Figure 2C), 7 proteins (28%) showed no differences between groups (PKM2, GFAP, NEFL, NEFM, HSPD1, DPYSL2, and YWHAG) whereas increased lipoxidation occurred in the 18 remaining proteins (72%) in older cases (CKB, GAPDH, PGAM1, ENO1, ACO2, ATP5A1, DLD, TPPP, PARK7, CRYAB, GOT1, BASP1, HBA1, CA1, BLVRB, PEBP1, SYN1, and UCHL1).

The most frequently lipoxidized proteins, accounting for at least 70% of cases, were GFAP (100%), HSPD1 (100%), CKB (93.33%), GAPDH (93.33%), NEFL (93.33%), NEFM (80%), DPYSL2 (80%), DLD (73.33%), PEBP1 (70%), and SYN1 (70%). Considering the cumulative presence of lipoxidized proteins by age group (Figure 2D), lipoxidation of specific proteins in all the regions increased in old-aged individuals. In the PC, values of cumulative count varied from 48 in middle-aged to 67 in old-aged cases. In FC, values varied from 79 in middle-aged to 107 in old-aged; whereas in the CG, there were 76 in middle-aged and 104 in old-aged individuals.

Quantification of selected lipoxidized protein levels

To determine whether increased lipoxidation of certain proteins might not be merely the result of the increased expression levels of that particular protein, selected protein levels were quantified. Proteins with no differences in any region (GFAP, NEFL, NEFM and HSPD1) were excluded. Proteins for which no commercial antibodies wee available (PKM2, DPYSL2, DLD, PEBP1, SYN1, GOT1, PGAM1, ACO2, TPPP, CA1 and BLVRB) were not analyzed. Finally, six lipoxidized proteins with increased cumulative levels of lipoxidation in old aged cases at least in two regions were assessed using 1D SDS-PAGE electrophoresis and western blotting with specific available antibodies: ATP5A1, CKB, ENO1, GAPDH, YWHAG and UCHL1. Quantification of the bands was carried out by densitometry (Supplementary Figure 2). Protein levels were compared between age in each region after checking normality of variables (non-normal data: ATP5A1 in PC; ENO1 and HBA1 in FC; and UCHL1 in CG). Statistical results of these

comparisons are summarized in Supplementary Table 2, and graphically represented in Supplementary Figure 3. There were no significant differences in the total expression levels of assessed proteins in any region when comparing middle-aged and old-aged groups, excepting significant decreased levels of YWHAG ($p < 0.02$) in the FC in the old-aged group, thus indicating that increased lipoxidation levels of defined proteins were not the result of increased expression of the corresponding total protein.

Characterization of lipoxidized proteins

To learn about the commonalities of proteins vulnerable to lipoxidation, their structures were analyzed using PredictProtein web-based software. The structural characteristics are represented in Figure 3.

Excluding BASP1, in which 100% is loop or disorganized, α-helix motive represents between 5.14 and 83.10%, β-strand represents between 1.2 and 31.43% (absent in NEFL and HBA1), and loops represent between 16.9 and 75.46% (Figure 3A). Proteins with secondary structures forming α-helix plus loops represent between 68.5% and 98.8%. Interestingly, exposure to the medium varied between 42.6% and 100%, and it was superior to 50% in 16 proteins (Figure 3B).

Regarding amino acid composition, the most common amino acids represented are alanine (mean frequency in the group: 9.71%), leucine (mean frequency in the group: 8.74%), and glycine (mean frequency in the group: 8.02%) as reported for the total pull of proteins present in Swiss-Prot database. However, the most frequent amino acids encountered in the exposed regions of lipoxidized proteins are lysine (mean frequency: 12.16%), glutamic acid (mean frequency: 11.44%), and aspartic acid (mean frequency: 8.53%) (Figure 3C).

With respect to the cellular location, analysis of GO term “cellular component” annotation revealed that the best represented sub-cellular localizations of lipoxidized proteins were cytoplasm, cytoskeleton, mitochondrion, and exosome. For the GO term “molecular function” lipoxidized proteins over-represented terms are binding, catalytic activity, and structural molecule.

Interactions of these proteins were explored using the STRING web-based tool. The network of interactions used for the analysis with a high confidence level of combined score computed and no more than 10 external partners is shown in Figure 4. Interestingly, the central node of the resulting network is occupied by ubiquitin.

The over-represented functional pathways in which lipoxidized proteins are involved were explored using Cytoscape software. The results from this analysis are presented in Figure 5 showing a high representation of GO term for processes related with energy metabolism (including glycolysis and gluconeogenesis, citric acid cycle, mitochondrial respiration, and rapid energy production), intermediate filament based process, axon cargo transport, cytoskeleton-dependent intracellular transport, protein stabilization, mitochondrial protein import, and carbon-oxygen lyase activity. Roughly 32% of lipoxidized proteins are involved in energy metabolism (CKB, GAPDH, PGAM1, ENO1, PKM2, ACO2, ATP5A1, and DLD), 16% in cytoskeleton-related functions (GFAP, NEFL, NEFM, and TPPP), 16% in proteostasis (HSPD1, PARK7, CRYAB, and UCHL1), 24% in neurotransmission directly or indirectly (PEBP1, SYN1, GOT1, DPYSL2, BASP1, and YWHAG), and the remaining 8% and 4% in O_2/CO_2 (HBA1 and CA1) and heme-group metabolism (BLVRB), respectively.

Soluble oligomers and NKT levels

The levels of soluble oligomers as revealed with the A11 antibody (Figure 6A) and NKT (Figure 6B) were detected with slot-blot densitometric analysis comparing middle-aged versus old-aged cases in every region using Student's t-test. Soluble oligomer levels were significantly increased in the older group with respect to middle-aged cases in the PC ($t = -2.83$, $p < 0.01$) and FC ($t = -3.98$, $p < 0.001$), whereas, no significant differences were found between age groups in the CG. With respect to NKT, only significantly increased levels ($t = -3.32$, $p < 0.005$) were found in the old-aged group when compared with middle-aged cases in the FC.

The same pattern was found when results were analyzed for significant continuous relations with age (Pearson's correlation). Positive significant correlations with age for oligomers in PC ($r = 0.52$, $p < 0.045$), for oligomers ($r = 0.65$, $p < 0.008$), and for NKT ($r = 0.57$, $p < 0.025$) in FC (Figure 6C). No correlation was found with age in the CG.

Significant positive correlations were seen between oligomers and NKT levels present in each one of the explored regions (PC: $r = 0.70$, $p < 0.004$; FC: $r = 0.89$, $p < 0.000$; CG: $r = 0.86$, $p < 0.000$), which are represented in Figure 7A.

To reduce dimensionality while preserving the maximum amount of information to infer significant associations between variables, Principal Components Analysis was used including oligomers and NKT levels for each region as active variables and age as supplementary variable (Figure 7B). Two principal components explained 83.18% of the variance in the data, the first component (Factor1: 52.49% of the variance) with a high information contribution from oligomer and NKT levels in PC and FC, and the second component (Factor 2: 30.69% of the variance) with information from oligomer and NKT levels in CG. Both factors were negatively correlated to age, but factor 1 showed a closer relation than factor 2. The projection of variables in the factor-plane graph summarizes this information, showing the closer positive relation of soluble oligomers and NKT levels in PC and FC among them and with age, and the more distant pattern of oligomers and NKT levels in CG.

Discussion

Protein lipoxidation in human cerebral cortex occurs at middle age and increases with physiological senescence

Cases analyzed were considered normal individuals with no neurological or mental diseases and with no neuropathological alterations excepting stage I of Braak and Braak and moderate status cribosus in some older cases. About 80% of individuals aged 65 years have neurofibrillary tangles in the entorhinal and transentorhinal cortices [34]. Factors other than age that might have interfered with the analysis of oxidized proteins, such as metabolic diseases and hypoxia were ruled out. Causes of death were similar in the two groups of cases. Post-mortem delay was within the range of feasibility [27]. Finally, the NKT antibody has been used and validated in previous studies [28-30].

Twenty-five NKT-adducted proteins were identified in the cerebral cortex of normal middle-aged and old-aged individuals. Four proteins, GFAP, NEFL, NEFM, and HSPD1, showed the same cumulative presence of NKT-adducted forms in the three regions and in both age groups. Some proteins having the same cumulative levels of NKT adducted forms in both age groups were identified in distinct regions: ATP5A1, DLD, BASP1, and SYN1 in PC; GAPDH and CKB in the FC; and PKM2, DPYSL2, and

YWHAG in the CG. However, adducted forms of all these proteins in a particular region increased in the other two regions in old-aged individuals.

The degree of lipoxidation of the vast majority of remaining proteins identified by the accumulation of NKT adducts was higher in old-aged individuals when compared to middle-aged cases in spite of regional variations. These proteins are PGAM1, ENO1, ACO2, TPPP, PARK7, CRYAB, GOT1, HBA1, CA, BLVRB, PEBP1, and UCHL1. However, certain proteins were lipoxidized only in old-aged individuals in certain regions such as PKM2, HBA1, and CA in the PC, and HBA1 in the FC.

Together, these observations show, on the one hand, that the cerebral cortex in individuals aged between 40 and 48 years contains lipoxidized proteins the levels of which vary from one region to another, and, on the other hand, that cumulative presence of NKT adducted forms increases in individuals aged between 70 and 79 years.

Importantly, increased lipoxidation is not related to increased levels of the corresponding protein but rather to increased vulnerability to lipoxidation with age as revealed by the higher values of oxidation compared with preserved total levels of the same protein.

Selective protein lipoxidation in human cerebral cortex

Susceptibility to lipoxidation is not uniform in all proteins [14, 35]. Assuming that ROS act stochastically, several factors can influence this specificity beyond abundance including structure, location, and functional characteristics. Localization of proteins, a particular cell type or subcellular compartment, may make them more vulnerable as a result of their environmental conditions [36]. An example of cell type-related vulnerability is GFAP localized in astrocytes which are the main brain producers of DHA [37] and its peroxidation derivatives. Regarding subcellular localization, HSPD1 and DLD are located in the mitochondria, the principal source of ROS [38]. NEFL and NEFM are proteins of the cytoskeleton, as well as DPYSL2 which is also located in the growth cones; PEBP1 is involved in neurotransmission and SYN1 is present in synaptic vesicles. It is worth stressing that axons and synaptic terminals have high energy demands achieved by continuous mitochondrial activity and recruitment, and rapid energy transduction mediated by CKB. In addition, axons are radial structures with a small diameter in comparison with the cell body which increases the probability of stochastic interactions between ROS and membrane lipids, thus propitiating lipid peroxidation.

The present findings also show that certain structural traits, mainly the presence of alpha helices and loops, render proteins susceptible to oxidative damage. Excepting cytoskeletal proteins, the rest of the proteins identified as targets of lipoxidation (excluding BASP1 which is completely disordered) are globular and form soluble coiled-shaped molecules with hydrophobic groups at the core and exposed hydrophilic groups. Moreover, proteins with the revealed amino acids lysine, glutamic acid, and aspartic acid are also particularly vulnerable; the average level of exposure is greater than 50% in sixteen proteins.

Functional clustering of oxidatively-damaged proteins

Principal systems affected by protein lipoxidation, considering the number of identified damaged proteins, are energy metabolism, cytoskeleton, proteostasis, neurotransmission, and O_2/CO_2 and heme metabolism.

There is strong evidence that energy metabolism is particularly affected during aging and neurodegeneration [8, 11, 17]. The present observations give some clues about the molecular substrates of energy failure with aging after the identification of key proteins as targets of lipoxidative damage, including proteins of the glycolysis GAPDH, PGAM1, ENO1, and PKM2; proteins of the citric acid cycle ACO2 and DLD; and ATP5A1 subunit of the respiratory mitochondrial complex V. All of them are components of coupled processes necessary to fulfill ATP requirements of cells. Neuronal activity is highly dependent on these processes since, under normal conditions, glucose is the exclusive energy substrate for the brain [39]. In addition, CKB is in charge of rapid ATP production from phosphocreatine reservoirs in response to acute increased energy demands in neurons, but CKB is also a key player in the 'phosphocreatine circuit' for cellular energy homeostasis [40]. Thus CKB provides neurons with a reservoir and also an alternative source of ATP from glycolysis, citric acid cycle, and respiration.

Cytoskeletal GFAP, NEFL, and NEFM are filamentous proteins composed of long parallel chains, linked by disulphide cross bridges, making the proteins very stable and prone to long half-lives. The present results are in line with previous observations showing that neurofilaments are major targets of 4-hydroxinonenal adduction (another marker of lipid peroxidation that covalently links lysine) in mice nervous system [41, 42]. They also support the concept that oxidation of certain cytoskeletal proteins is under a tightly regulated mechanism of redox control during life-span [41]. Whether these changes do occur in the same direction in other brain regions is not known; nor is the functional implication of the high constant levels of oxidation of GFAP, NEFL, and NEFM in the three regions examined of the cerebral cortex understood. Moreover, a certain degree of lipoxidation in selected cytoskeletal proteins turns out perhaps to be useful for the normal functioning of the cytoskeleton. Whether possible disturbances of tubulin polymerization result from increased NKT adducts with aging in TPPP remains speculative.

Oxidation of chaperones involves mitochondrial (HSPD1) and cytosolic (CRYAB) molecules. HSPD1 modulates protein import and folding into the mitochondria [43]; CRYAB exhibits chaperone-like activity, and is able to prevent protein aggregation during stress situations while also increasing the resistance of cells to oxidative injuries [44]. PARK7 is a redox-dependent chaperone that reduces intracellular ROS through oxidation of itself [45], maintains mitochondrial homeostasis [46], and regulates gene transcription [47].

Regarding oxidized proteins linked to neurotransmission, PEBP1 modulates choline acetyltransferase during acetylcholine synthesis [48]. Phosphoprotein SYN1 coats synaptic vesicles, modulating synaptic vesicle release, synaptic transmission, and plasticity [49]. GOT1 participates in the synthesis and regulation of the levels of glutamate [50], the neurotransmitter responsible for around 90% of the excitatory synapsis on the brain. BASP1 is found in nerve terminals, enriched in synaptic vesicles and in the lipid raft fraction of synaptic plasma membranes [51]; BASP1 regulates the transport of glutamic acid decarboxylases to the presynaptic terminals and their anchoring to the synaptic vesicles [52. DPYSL2 has relevant functions in axon guidance and neurite outgrowth, as well as in synaptic vesicle and N-methyl-Daspartate glutamate receptor trafficking [53]. YWHAG is a member of the 14-3-3 group of proteins which display a plethora of functions, among them the ability to activate tryptophan and tyrosine hydroxylases, the rate-limiting enzymes in the

synthesis of serotonin and catecholamines, respectively [54]. These modifications together with those linked to the high energy demands make synapses especially vulnerable to oxidative stress damage.

Three proteins related to heme metabolism and O_2 and CO_2 regulation, BLVRB, CA and HB1A, are also oxidatively damaged. CA participates in the conversion of CO_2 into bicarbonate and participates in the transport of CO_2 out of the tissues. BLVDR regulates the final step in heme metabolism, but it also regulates glucose metabolism and has neuroprotective effects [55]. HBA1 is a component of haemoglobin whose role in the nervous system is still poorly understood. Haemoglobin has been found in neurons where it probably plays a role in O_2 transport or as a regulator of cytosolic neuronal O_2 [56]. Interestingly, haemoglobin levels are reduced in neurons in AD [57]. Oxidative damage of, at least, those three proteins tags cell O_2 and CO_2 regulation as a target of putative cellular respiratory dysfunction in the elderly.

Finally, molecular interactions of lipoxidized proteins in the human cerebral cortex were explored to identify systems that may be indirectly impaired as a result of primary protein lipoxidation and presumable loss of function. Ubiquitin C has been identified as the central node of the network of interactions. Ubiquitin conjugation to proteins plays a cardinal role in the ubiquitin-proteasome system and protein turnover which has been identified as being affected in neurodegenerative diseases associated with aging [58]. Since ubiquitin conjugation to target proteins occurs through the ε-amino group of lysine, NKT adduction of this group can restrain protein-ubiquitin interactions and then hamper the degradation of altered proteins. In addition, 50% of the ubiquitin binding sites are not involved in protein degradation by the ubiquitin-proteasome system [59], suggesting that ubiquitin serves other molecular pathways. If true, several pathways can be deregulated as a result of altered ubiquitin conjugation with oxidized proteins.

NKT adduction and soluble oligomers

Aberrant protein structures are able to generate soluble oligomers; such molecular species are increasingly recognized for their high cytotoxic potential [22, 60]. Soluble oligomers have been detected by using the structure-specific amino acid sequence independent antibody A11 [23]. Therefore, although initially generated to recognize β-amyloid soluble oligomers, undefined oligomeric species can be detected as well.

NKT adduction of proteins generates aberrant structures like crosslinking and aggregation [19]. For this reason, global levels of protein NKT adduction and the presence of oligomers have been analyzed in every sample. A positive significant relation is found between protein NKT and soluble oligomer levels in the three cortical regions assessed, suggesting that modifications of proteins resulting from NKT adduction parallel soluble oligomer formation. Levels of oligomers increase with age in the PC and FC, and NKT levels significantly increase with age just in FC, whereas at CG total NKT and oligomer levels showed no differences between age groups.

The present findings also complement previous observations showing increased levels of soluble oligomers in the entorhinal and frontal cortices when comparing middle-aged individuals lacking AD related pathology with older cases with AD-related pathology stages I-II. Thus, increased levels of soluble oligomers are indeed a characteristic feature of the aging human brain coincidental with first stages of AD-related pathology [61]. Importantly, increased levels of oligomeric species parallel expression levels of brain cytokines and mediators of the immune response in old age [61]. Whether these

coincidences have a cause-effect relationship needs further study using appropriate *in vitro* and *in vivo* models.

Implications on regional brain functions

The present observations may have implications in brain function. FC area 8, a part of the dorsolateral prefrontal cortex, participates in executive functions in connection with other brain regions including PC [62, 63]. PC area 7 is also linked to several high-level processing tasks [64]. Interestingly, the molecular relationship found between PC and FC complements findings from tractography showing an anterior-posterior gradient in age-related white matter degradation of specific long-range white matter tracts connecting FC and PC [64]. In the same study, reduced frontal tract integrity correlated with reduced executive and working memory functions. This accounts, at least in part, for cognitive performance decline in older adults. Interconnection of FC and PC is also important in the elderly as in healthy old-aged subjects PC is compensatorily recruited to perform frontal cortex cognitive tasks [65]. Analysis of the principal components in the present study reveals similar patterns of protein oxidation and oligomer burden in PC and FC, and relative independence of the CG during aging.

CG area 23 has a central role in supporting internally-directed cognition. It is a key component of the default mode network which is involved in self-referential functions and is highly correlated with activity at rest [66]. The posterior CG exhibits a transitional pattern of connectivity coordinating distinct networks for efficient cognitive function [67]. In line, posterior CG presents a striking high rate of metabolism: cerebral blood flow and metabolic rate are around 40% greater than average within the region in human brain [68]. Reduced metabolism in this region is accompanied by reduced CG functional connectivity [69].

Conclusions

Together, the present findings provide information about increased protein damage by lipoxidation with aging, which may compromise vital cell functions such as energy metabolism, cytoskeleton, proteostasis, neurotransmission, O_2/CO_2, and heme homeostasis. Post-translationally modified proteins resulting from oxidative damage, in addition to certain oligomeric species, truncated proteins, lipids, and metabolites, can be considered as putative collaborative factors contributing to neuronal senescence. Protein vulnerability to oxidation is related to the particular sub-cellular localization of certain proteins, the secondary structure of the protein, and the external exposure of certain amino acids which are more vulnerable to lipoxidation. Increased oxidative damage of key proteins in the FC, PC and CG may impact on normal brain function particularly in cognition, integrative connectivity and coordination of activation-rest responses in brain. Importantly, since lipoxidative damage to proteins is already identified in normal middle-aged individuals and it increases physiologically in the elderly, it seems reasonable to act upon the appropriate ROS-producer targets at the befitting middle-age window.

Acknowledgements

This study was funded by the Seventh Framework Programme of the European Commission, grant agreement 278486: DEVELAGE, and by the Ministerio de Ciencia e Innovación, Instituto de Salud Carlos III – Fondos FEDER, a way to build Europe FIS grants PI14/00757 and PI14/00328. We wish to thank T. Yohannan for editorial help.

Conflict of interest

No relevant data

References

Journal:
[1] Muller, F. L.; Lustgarten, M. S.; Jang, Y.; Richardson, A.; Van Remmen, H. Trends in oxidative aging theories. Free Radic. Biol. Med. 43:477-503; 2007.

[1] T.B.L. Kirkwood, Understanding the odd science of aging, Cell. 120 (2005) 437–47.

[2] T.C. Goldsmith, An Introduction to Biological Aging Theory, Azinet Press, Crownsville, 2011.

[3] M.J. West, Age-related neuronal loss in the cerebral cortex, in: A. Peters, J.H. Morrison (Eds.), Cerebral Cortex vol 14 Neurodegenerative and age-related changes in structure and function of cerebral cortex, Kluwer Academic/Plenum Press, New York, Boston, Dordrecht, London, Moscow, 1999, pp. 81–8.

[4] D.L. Rosene, T.J. Nicholson, Neurotransmitter receptor changes in the hippocampus and cerebral cortex in normal aging, in: A. Peters, J.H. Morrison (Eds.), Cerebral Cortex vol 14 Neurodegenerative and age-related changes in structure and function of cerebral cortex, Kluwer Academic/Plenum Press, New York, Boston, Dordrecht, London, Moscow, 1999, pp. 111–28.

[5] P.R. Hof, J.H. Morrison, The aging brain: morphomolecular senescence of cortical circuits, Trends Neurosci. 27 (2004) 607–13.

[6] M.M. Esiri, Ageing and the brain, J. Pathol. 211 (2007) 181–7.

[7] M.P. Mattson, T. Magnus, Ageing and neuronal vulnerability, Nat. Rev. Neurosci. 7 (2006) 278–94.

[8] D. Harman, Aging: overview, Ann. N. Y. Acad. Sci. 928 (2001) 1–21.

[9] S.K. Kim, Common aging pathways in worms, flies, mice and humans, J. Exp. Biol. 210 (2007) 1607–12.

[10] T.M. Hagen, Oxidative stress, redox imbalance, and the aging process, Antioxid. Redox Signal. 5 (2003) 503–6.

[11] M. Jové, M. Portero-Otín, A. Naudí, I. Ferrer, R. Pamplona, Metabolomics of human brain aging and age-related neurodegenerative diseases, J. Neuropathol. Exp. Neurol. 73 (2014) 640–57.

[12] A. Naudí, R. Cabré, M. Jové, V. Ayala, H. Gonzalo, M. Portero-Otín, et al., Lipidomics of human brain aging and Alzheimer's disease pathology, Int. Rev. Neurobiol. 122 (2015) 133–89.

[13] R. Pamplona, E. Dalfó, V. Ayala, M.J. Bellmunt, J. Prat, I. Ferrer, et al., Proteins in human brain cortex are modified by oxidation, glycoxidation, and lipoxidation. Effects of Alzheimer disease and identification of lipoxidation targets, J. Biol. Chem. 280 (2005) 21522–30.

[14] A. Martínez, M. Portero-Otin, R. Pamplona, I. Ferrer, Protein targets of oxidative damage in human neurodegenerative diseases with abnormal protein aggregates, Brain Pathol. 20 (2010) 281–97.

[15] A. Nunomura, P.I. Moreira, R.J. Castellani, H.G. Lee, X. Zhu, M.A. Smith, et al., Oxidative damage to RNA in aging and neurodegenerative disorders, Neurotox. Res. 22 (2012) 231–48.

[16] R.X. Santos, S.C. Correia, X. Zhu, M.A. Smith, P.I. Moreira, R.J. Castellani, et al., Mitochondrial DNA oxidative damage and repair in aging and Alzheimer's disease, Antioxid. Redox Signal. 18 (2013) 2444–57.

[17] R. Pamplona, G. Barja, Mitochondrial oxidative stress, aging and caloric restriction: the protein and methionine connection, Biochim. Biophys. Acta - Bioenerg. 1757 (2006) 496–508.

[18] J.S. O'Brien, E.L. Sampson, Lipid composition of the normal human brain: gray matter, white matter, and myelin, J. Lipid Res. 6 (1965) 537–44.

[19] N. Bernoud-Hubac, S.S. Davies, O. Boutaud, T.J. Montine, L.J. Roberts, Formation of highly reactive γ-ketoaldehydes (neuroketals) as products of the neuroprostane pathway, J. Biol. Chem. 276 (2001) 30964–70.

[20] N. Bernoud-Hubac, L.J. Roberts, Identification of oxidized derivatives of neuroketals, Biochemistry. 41 (2002) 11466–71.

[21] D.A. Butterfield, J. Kanski, Brain protein oxidation in age-related neurodegenerative disorders that are associated with aggregated proteins, Mech. Ageing Dev. 122 (2001) 945–62.

[22] M.J. Guerrero-Muñoz, D.L. Castillo-Carranza, R. Kayed, Therapeutic approaches against common structural features of toxic oligomers shared by multiple amyloidogenic proteins, Biochem. Pharmacol. 88 (2014) 468–78.

[23] C.G. Glabe, Conformation-dependent antibodies target diseases of protein misfolding, Trends Biochem. Sci. 29 (2004) 542–7.

[24] R. Kayed, E. Head, J.L. Thompson, T.M. McIntire, S.C. Milton, C.W. Cotman, et al., Common structure of soluble amyloid oligomers implies common mechanism of pathogenesis, Science. 300 (2003) 486–9.

[25] I. Dalle-Donne, A. Scaloni, D.A. Butterfield, Redox Proteomics: From protein modifications to cellular dysfunction and diseases, Wiley Interscience, New Jersey, 2006.

[26] M. Perluigi, A.M. Swomley, D.A. Butterfield, Redox proteomics and the dynamic molecular landscape of the aging brain, Ageing Res. Rev. 13 (2014) 75–89.

[27] I. Ferrer, A. Martinez, S. Boluda, P. Parchi, M. Barrachina, Brain banks: benefits, limitations and cautions concerning the use of post-mortem brain tissue for molecular studies, Cell Tissue Bank. 9 (2008) 181–94.

[28] E.V. Ilieva, V. Ayala, M. Jové, E. Dalfó, D. Cacabelos, M. Povedano, M.J. Bellmunt, I. Ferrer,R. Pamplona, M. Portero-Otín M, Oxidative and endoplasmic reticulum stress interplay in sporadic amyotrophic lateral sclerosis, Brain. 130 (2007) 3111-23.

[29] A. Kichev, E.V. Ilieva, G. Piñol-Ripoll, P. Podlesniy, I. Ferrer, M. Portero-Otín, R. Pamplona, C. Espinet C, Cell death and learning impairment in mice caused by in vitro modified pro-NGF can be related to its increased oxidative modifications in Alzheimer disease. Am J Pathol. 175 (2009) 2574-85.

[30] H. Gonzalo, L. Brieva, F. Tatzber, M. Jové, D. Cacabelos, A. Cassanyé, et al. Lipidome analysis in multiple sclerosis reveals protein lipoxidative damage as a potential pathogenic mechanism. J Neurochem. 123 (2012): 622-34.

[31] A. Franceschini, D. Szklarczyk, S. Frankild, M. Kuhn, M. Simonovic, A. Roth, et al., STRING v9.1: protein-protein interaction networks, with increased coverage and integration, Nucleic Acids Res. 41 (2013) D808–15.

[32] G. Bindea, B. Mlecnik, H. Hackl, P. Charoentong, M. Tosolini, A. Kirilovsky, et al., ClueGO: a Cytoscape plug-in to decipher functionally grouped gene ontology and pathway annotation networks, Bioinformatics. 25 (2009) 1091–3.

[33] G. Bindea, J. Galon, B. Mlecnik, CluePedia Cytoscape plugin: pathway insights using integrated experimental and in silico data, Bioinformatics. 29 (2013) 661–3.

[34] I. Ferrer, Defining Alzheimer as a common age-related neurodegenerative process not inevitably leading to dementia, Prog. Neurobiol. 97 (2012) 38–51.

[35] J. Petrak, R. Ivanek, O. Toman, R. Cmejla, J. Cmejlova, D. Vyoral, et al., Déjà vu in proteomics. A hit parade of repeatedly identified differentially expressed proteins, Proteomics. 8 (2008) 1744–9.

[36] M. Eisenstein, Location, location, location, Nat. Methods. 6 (2009) 630–1.

[37] W.J. Lukiw, N.G. Bazan, Docosahexaenoic acid and the aging brain, J. Nutr. 138 (2008) 2510–4.

[38] A.A. Starkov, Measurement of mitochondrial ROS production, Methods Mol. Biol. 648 (2010) 245–55.

[39] P.J. Magistretti, Cellular bases of functional brain imaging: insights from neuron-glia metabolic coupling, Brain Res. 886 (2000) 108–12.

[40] T. Wallimann, M. Wyss, D. Brdiczka, K. Nicolay, H.M. Eppenberger, Intracellular compartmentation, structure and function of creatine kinase isoenzymes in tissues with high and fluctuating energy demands: the “phosphocreatine circuit” for cellular energy homeostasis, Biochem. J. 281(Pt 1) (1992) 21–40.

[41] T. Wataya, A. Nunomura, M.A. Smith, S.L. Siedlak, P.L.R. Harris, S. Shimohama, et al., High molecular weight neurofilament proteins are physiological substrates of adduction by the lipid peroxidation product hydroxynonenal, J. Biol. Chem. 277 (2002) 4644–8.

[42] E.A. Perry, R.J. Castellani, P.I. Moreira, A. Nunomura, Q. Lui, P.L.R. Harris, et al., Neurofilaments are the major neuronal target of hydroxynonenal-mediated protein cross-links, Free Radic. Res. 47 (2013) 507–10.

[43] S.A. Broadley, F.U. Hartl, The role of molecular chaperones in human misfolding diseases, FEBS Lett. 583 (2009) 2647–53.

[44] Simon S, Arrigó P. Small Stress Proteins and Human Diseases, Nova Biomedical Inc., New York, 2010.

[45] S. Shendelman, A. Jonason, C. Martinat, T. Leete, A. Abeliovich, DJ-1 is a redox-dependent molecular chaperone that inhibits alpha-synuclein aggregate formation, PLoS Biol. 2 (2004) e362.

[46] C. Chang, G. Wu, P. Gao, L. Yang, W. Liu, J. Zuo, Upregulated Parkin expression protects mitochondrial homeostasis in DJ-1 konckdown cells and cells overexpressing the DJ-1 L166P mutation, Mol. Cell. Biochem. 387 (2014) 187–95.

[47] C.M. Clements, R.S. McNally, B.J. Conti, T.W. Mak, J.P.Y. Ting, DJ-1, a cancer and Parkinson’s disease-associated protein, stabilizes the antioxidant transcriptional master regulator Nrf2, Proc. Natl. Acad. Sci. U. S. A. 103 (2006) 15091–6.

[48] K. Ojika, Y. Tsugu, S. Mitake, Y. Otsuka, E. Katada, NMDA receptor activation enhances the release of a cholinergic differentiation peptide (HCNP) from hippocampal neurons in vitro, Brain Res. Dev. Brain Res. 106 (1998) 173–80.

[49] P. Farisello, D. Boido, T. Nieus, L. Medrihan, F. Cesca, F. Valtorta, et al., Synaptic and extrasynaptic origin of the excitation/inhibition imbalance in the hippocampus of synapsin I/II/III knockout mice, Cereb. Cortex. 23 (2013) 581–93.

[50] C. Rink, S. Gnyawali, L. Peterson, S. Khanna, Oxygen-inducible glutamate oxaloacetate transaminase as protective switch transforming neurotoxic glutamate to metabolic fuel during acute ischemic stroke, Antioxid. Redox Signal. 14 (2011) 1777–85.

[51] M.I. Mosevitsky, Nerve ending "signal" proteins GAP-43, MARCKS, and BASP1, Int. Rev. Cytol. 245 (2005) 245–325.

[52] S. Maekawa, Y. Kobayashi, S.I. Odagaki, M. Makino, H. Kumanogoh, S. Nakamura, et al., Interaction of NAP-22 with brain glutamic acid decarboxylase (GAD), Neurosci. Lett. 537 (2013) 50–4.

[53] D. Martins-de-Souza, J.S. Cassoli, J.M. Nascimento, K. Hensley, P.C. Guest, A.M. Pinzon-Velasco, et al., The protein interactome of collapsin response mediator protein-2 (CRMP2/DPYSL2) reveals novel partner proteins in brain tissue, Proteomics. Clin. Appl. 9 (2015) 817–31.

[54] P. Steinacker, A. Aitken, M. Otto, 14-3-3 proteins in neurodegeneration, Semin. Cell Dev. Biol. 22 (2011) 696–704.

[55] D.E. Baranano, M. Rao, C.D. Ferris, S.H. Snyder, Biliverdin reductase: a major physiologic cytoprotectant, Proc. Natl. Acad. Sci. U. S. A. 99 (2002) 16093–8.

[56] M. Biagioli, M. Pinto, D. Cesselli, M. Zaninello, D. Lazarevic, P. Roncaglia, et al., Unexpected expression of alpha- and beta-globin in mesencephalic dopaminergic neurons and glial cells, Proc. Natl. Acad. Sci. U. S. A. 106 (2009) 15454–9.

[57] I. Ferrer, A. Gómez, M. Carmona, G. Huesa, S. Porta, M. Riera-Codina, et al., Neuronal hemoglobin is reduced in Alzheimer's disease, argyrophilic grain disease, Parkinson's disease, and dementia with Lewy bodies, J. Alzheimers Dis. 23 (2011) 537–50.

[58] T. Hoppe, Life and destruction: ubiquitin-mediated proteolysis in aging and longevity, F1000 Biol. Rep. 2 (2010) 79.

[59] S.A. Wagner, P. Beli, B.T. Weinert, M.L. Nielsen, J. Cox, M. Mann, et al., A proteome-wide, quantitative survey of in vivo ubiquitylation sites reveals widespread regulatory roles, Mol. Cell. Proteomics. 10 (2011) M111.013284.

[60] C.G. Glabe, Common mechanisms of amyloid oligomer pathogenesis in degenerative disease, Neurobiol Aging. 27 (2006) 570–5.

[61] I. López-González, A. Schlüter, E. Aso, P. Garcia-Esparcia, B. Ansoleaga, F. Llorens, et al., Neuroinflammatory signals in Alzheimer disease and APP/PS1 transgenic mice: correlations with plaques, tangles, and oligomeric species, J. Neuropathol. Exp. Neurol. 74 (2015) 319–44.

[62] A.K. Barbey, R. Colom, J. Grafman, Dorsolateral prefrontal contributions to human intelligence, Neuropsychologia. 51 (2013) 1361–9.

[63] A.E. Cavanna, M.R. Trimble, The precuneus: a review of its functional anatomy and behavioural correlates, Brain. 129 (2006) 564–83.

[64] S.W. Davis, N.A. Dennis, N.G. Buchler, L.E. White, D.J. Madden, R. Cabeza, Assessing the effects of age on long white matter tracts using diffusion tensor tractography, Neuroimage. 46 (2009) 530–41.

[65] C.M. Huang, T.A. Polk, J.O. Goh, D.C. Park, Both left and right posterior parietal activations contribute to compensatory processes in normal aging, Neuropsychologia. 50 (2012) 55–66.

[66] R. Leech, D.J. Sharp, The role of the posterior cingulate cortex in cognition and disease, Brain. 137 (2014) 12–32.

[67] R. Leech, S. Kamourieh, C.F. Beckmann, D.J. Sharp, Fractionating the default mode network: distinct contributions of the ventral and dorsal posterior cingulate cortex to cognitive control, J. Neurosci. 31 (2011) 3217–24.

[68] M.E. Raichle, A.M. MacLeod, A.Z. Snyder, W.J. Powers, D.A. Gusnard, G.L. Shulman, A default mode of brain function, Proc. Natl. Acad. Sci. U. S. A. 98 (2001) 676–82.

[69] T. Hedden, K.R.A. Van Dijk, J.A. Becker, A. Mehta, R.A. Sperling, K.A. Johnson, et al., Disruption of functional connectivity in clinically normal older adults harboring amyloid burden, J. Neurosci. 29 (2009) 12686–94.

Tables

Table 1: Cases examined in the present series

Case	Age (years)	Group	Gender	Cause of death	Post-mortem delay	Neuropathology	2D	1D	Slot-Blot
1	40	Middle-aged	Female	CA	8h 45min	NL	X	X	-
2	40	Middle-aged	Male	PNEU	5h 10min	NL	X	X	X
3	44	Middle-aged	Male	THR_EMB	6h 40min	NL	X	X	-
4	45	Middle-aged	Male	C-INF	4h 5min	CRIB	X	X	X
5	46	Middle-aged	Female	MYO	7h 15min	CRIB	X	X	X
6	48	Middle-aged	Female	CA	4h 5min	NL	-	X	X
7	52	Middle-aged	Male	PNEU	9h 30min	NL	-	X	X
8	52	Middle-aged	Male	C-INF	4h 40min	NL	-	X	X
9	57	Middle-aged	Male	PNEU	5h 20min	NL	-	X	X
10	61	Old-aged	Male	CA	4h 30min	AD I	-	X	X
11	65	Old-aged	Male	CA	3h 15min	AD I	X	X	X
12	66	Old-aged	Male	THR-EMB	6h 25min	NL	-	X	X
13	67	Old-aged	Male	CA	14h 40min	AD I	-	X	X
14	70	Old-aged	Male	CA	2h	AD I	-	X	X
15	75	Old-aged	Female	C-INF	6h 10min	AD I	X	X	X
16	76	Old-aged	Male	PNEU	6h 30min	AD I	X	X	X
17	77	Old-aged	Male	C-INF	6h 55min	AD I	X	X	X
18	79	Old-aged	Female	INT-INF	6h 25min	AD I	X	X	-

NL: no lesions; CRIB: status cribosus; AD I: Alzheimer disease-related pathology with Braak and Braak stage I of neurofibrillary degeneration; 2D: Two-dimensional electrophoresis; 1D: Mono-dimensional electrophoresis; CA: carcinoma; PNEU: pneumonia; C-INF: cardiac infarction; THR-EMB: pulmonary thrombosis-embolism; MYO: myocardioathy; INT-INF: intestinal infarction

Table 2: Identification of lipoxidized proteins with mass spectrometry

Spot	Protein	Swiss-prot Accession No.	Mascot Score	Coverage (%)	MW (kDa)	pI
1	Dihydropyrimidinase-related protein 2 (DPYSL2)	Q16555	724.28	48.43	62.25	6.38
2	Dihydropyrimidinase-related protein 2 (DPYSL2)	Q16555	1085.17	62.76	62.25	6.38
3	60 kDa heat shock protein, mitochondrial (HSPD1)	P10809	4087.37	83.60	61.02	5.87
4	60 kDa heat shock protein, mitochondrial (HSPD1)	P10809	2275.19	77.49	61.02	5.87
5	60 kDa heat shock protein, mitochondrial (HSPD1)	P10809	4285.96	89.35	61.02	5.87
6	60 kDa heat shock protein, mitochondrial (HSPD1)	P10809	2412.60	72.25	61.02	5.87
7	Glyceraldehyde-3-phosphate dehydrogenase (GAPDH)	P04406	1937.82	88.06	36.03	8.46
8	Glyceraldehyde-3-phosphate dehydrogenase (GAPDH)	P04406	1711.18	70.45	36.03	8.46
9	Glyceraldehyde-3-phosphate dehydrogenase (GAPDH)	P04406	2334.34	79.10	36.03	8.46
10	Glyceraldehyde-3-phosphate dehydrogenase (GAPDH)	P04406	842.06	43.28	36.03	8.46
11	Ubiquitin carboxyl-terminal hydrolase L1 (UCHL1)	P09936	1082.92	78.03	24.81	5.48
12	Protein DJ-1 (PARK7)	Q99497	625.43	89.42	19.88	6.79
13	Protein DJ-1 (PARK7)	Q99497	1262.00	89.42	19.88	6.79
14	Protein DJ-1 (PARK7)	Q99497	1065.72	85.71	19.88	6.79
15	Protein DJ-1 (PARK7)	Q99497	808.75	89.42	19.88	6.79
16	Alpha-crystallin B chain (CRYAB)	P02511	2069.68	97.14	20.15	7.53
17	Phosphatidylethanolamine-binding protein 1 (PEBP1)	P30086	2255.23	81.28	21.04	7.53
18	Neurofilament medium polypeptide (NEFM)	P07197	479.13	12.77	102.41	4.91
19	Neurofilament light polypeptide (NEFL)	P07196	902.93	41.25	61.47	4.65
20	Pyruvate kinase isozymes M1/M2 (PKM2)	P14618	860.77	42.94	57.90	7.84
21	Dihydrolipoyl dehydrogenase, mitochondrial (DLD)	P09622	337.68	25.34	54.14	7.85
22	Brain acid soluble protein 1 (BASP1)	P80723	800.65	81.50	22.68	4.63
23	Glial fibrillary acidic protein (GFAP)	P14136	1830.71	64.35	49.85	5.52
24	ATP synthase subunit alpha, mitochondrial (ATP5A1)	P25705	1447.00	46.65	59.71	9.13
25	Alpha-enolase (ENO1)	P06733	709.67	33.87	47.14	7.39
26	Alpha-enolase (ENO1)	P06733	728.28	41.71	47.14	7.39
27	Creatine kinase B-type (CKB)	P12277	724.17	56.96	42.62	5.59
28	Aspartate aminotransferase, cytoplasmic (GOT1)	P17174	1116.53	68.28	46.22	7.01
29	14-3-3 protein gamma (YWHAG)	P61981	1494.57	80.97	28.28	4.89
30	Hemoglobin subunit alpha (HBA1)	P69905	1400.82	85.21	15.25	8.68
31	Synapsin-1 (SYN1)	P17600	315.53	32.06	74.07	9.83
32	Aconitate hydratase, mitochondrial (ACO2)	Q99798	606.55	34.36	85.37	7.61
33	Dihydrolipoyl dehydrogenase, mitochondrial (DLD)	P09622	504.52	28.29	54.14	7.85
34	Alpha-enolase (ENO1)	P06733	2341.02	55.53	47.14	7.39
35	Carbonic anhydrase 1 (CA1)	P00915	481.65	52.49	28.85	7.12
36	Phosphoglyceratemutase 1 (PGAM1)	P18669	261.15	65.75	28.79	7.18
37	Tubulin polymerization-promoting protein (TPPP)	O94811	528.08	36.07	23.68	9.44
38	NADPH-Flavin reductase (BLVRB)	P30043	323.79	42.23	22.11	7.65
39	Phosphatidylethanolamine-binding protein 1 (PEBP1)	P30086	466.32	48.13	21.04	7.53

Table 3: Lipoxidized proteins: localization and functions

Protein	Main localization	Functions
		Energy metabolism
Creatine kinase B-type (CKB)	Cytosol, EVE	Energy transduction
Glyceraldehyde-3-phosphate dehydrogenase (GAPDH)	Cytosol, cytoskeleton, nucleus, EVE	Glycolysis (step 6); nuclear functions; organization of cytoskeleton
Phosphoglyceratemutase 1 (PGAM1)	Cytosol, EVE	Glycolysis (step 8); regulates anabolic biosynthesis
Alpha-enolase (ENO1)	Cytosol, membrane, nucleus, EVE	Glycolysis (step 9); growth control; hypoxia tolerance; immune responses
Pyruvate kinase isozymes M1/M2 (PKM2)	Cytosol, nucleus, EVE	Glycolysis (last step); linked to caspase-independent programmed cell death
Aconitate hydratase (ACO2)	Mitochondrion, nucleus	Catalyzes the isomerization of citrate to isocitrate within the tricarboxylic acid cycle
ATP synthase subunit alpha (ATP5A1)	Mitochondrion, EVE	Component of the ATP synthase complex which produces ATP during the oxidative phosphorylation
Dihydrolipoyl dehydrogenase (DLD)	Mitochondrion	Component of the pyruvate, α-ketoglutarate and branched-chain amino acid dehydrogenase complexes, and of the glycine cleavage system
		Cytoskeleton
Glial fibrillary acidic protein (GFAP)	Glial cytoskeleton - intermediate filament	Structural constituent of cytoskeleton; cell-specific marker that distinguishes astrocytes
Neurofilament light polypeptide (NEFL)	Cytoskeleton - neurofilament	Neuronal cytoskeleton; maintenance of neuronal caliber; axon cargo transport
Neurofilament medium polypeptide (NEFM)	Cytoskeleton - neurofilament	Neuronal cytoskeleton; maintenance of neuronal caliber; axon cargo transport
Tubulin polymerization-promoting protein (TPPP)	Cytoskeleton, nucleus, EVE	Integrity of microtubule network; mitotic spindle assembly and nuclear envelope breakdown
		Proteostasis
60 kDa heat shock protein, mitochondrial (HSPD1)	Mitochondrion, cytosol, EVE	Mitochondrial protein import and macromolecular assembly; folding of proteins; apoptotic process
Protein DJ-1 (PARK7)	Cytosol, nucleus, mitochondrion, EVE	Protects against oxidative stress and cell death; chaperone activity; pleotropic regulatory activities
Alpha-crystallin B chain (CRYAB)	Cytosol, nucleus, EVE	Chaperone-like activity; prevents aggregation of proteins under stress conditions
Ubiquitin carboxyl-terminal hydrolase L1 (UCHL1)	Cytosol, membrane, ER, EVE	Processing of ubiquitin precursors and ubiquitinated proteins
		Neurotransmission
Aspartate aminotransferase (GOT1)	Cytosol, nucleus, EVE	Biosynthesis of L-glutamate; regulator of glutamate levels; scavenger of glutamate in neuroprotection
Dihydropyrimidinase-related protein 2 (DPYSL2)	Cytosol, cytoskeleton, membrane, EVE	Neuronal development and polarity including axon growth and guidance, growth cone collapse and cell migration; synaptic vesicle trafficking
Phosphatidylethanolamine-binding protein 1 (PEBP1)	Cytosol nucleus, EVE	Binds ATP, opioids and phosphatidylethanolamine; inhibitor of serine proteases and RAF1 kinase activity
Synapsin-1 (SYN1)	Golgi apparatus, synaptic vesicle	Coats synaptic vesicles and regulates neurotransmitter release; pre-synaptic nitric oxid functions
Brain acid soluble protein 1 (BASP1)	Cytosol, membrane, nucleus, EVE	Protein and DNA binding; transcription regulatory activity; development regulation
14-3-3 protein gamma (YWHAG)	Cytosol, EVE	Regulation of a large spectrum of general and specialized signaling pathways
		O_2/CO_2/heme metabolism
Hemoglobin subunit alpha (HBA1)	Cytosol, EVE	Oxygen transport
Carbonic anhydrase 1(CA1)	Cytosol, EVE	Reversible hydration of CO_2; hydrates cyanamide to urea
NADPH-Flavin reductase (BLVRB)	Cytosol, membrane, nucleus, EVE	Oxidoreductase: catalyzes NADPH-dependent reduction of a variety of flavins; heme catabolism;

Note: Localization and functions based on the reported in the UniProt database (http://www.uniprot.org/). ER, endoplasmic reticulum; EVE, extracellular vesicular exosome. Proteins are separated into the groups: energy metabolism, cytoskeleton, proteostasis, neurotransmission, and O_2/CO_2 and heme metabolism.

Figure legends

Figure 1: Bi-dimensional (2D) gel electrophoresis and western blotting to neuroketal (NKT) of the parietal cortex (A), frontal cortex (B) and cingulate gyrus of two representative samples of middle-aged (40 years, left column) and old-aged (76 years, right column) individuals (corresponding to cases 1 and 16 in Table 1). Thirty nine spots (labeled in white numbers) were selected considering NKT adduction differences in all the cases analyzed for further identification by mass spectrometry.

Figure 2: Number of cases by age group with presence of neuroketal adducted forms of the twenty five selected proteins identified by redox proteomics in the parietal cortex (A), frontal cortex (B), cingulate gyrus (C) and cumulative counts of the three regions (D). Proteins are discriminated into clusters corresponding to energy metabolism, cytoskeleton, proteostasis, neurotransmission, and O_2/CO_2/heme metabolism. Number of cases with protein neuroketal adducts are higher in old-aged when compared with middle-aged individuals, but most oxidized proteins are already present in middle-aged individuals. Note that the cytoskeletal proteins GFAP, NEFL and NEFM, and the chaperone HSPD1 show the same level of oxidative modifications in middle-aged and old-aged individuals.

Figure 3: Structural characterization of the group of neuroketal-adducted proteins as revealed with the PredictProtein software analysis. Predominant structures of oxidized proteins are helix and loops (A). Most proteins have structures exposed to solvents (B). The most frequent amino acids exposed are lysine, glutamic acid and aspartic acid (C).

Figure 4: Protein-protein interactions networks derived from the STRING software analysis of the identified neuroketal-adducted proteins. Several robust interactions are encountered in the diagram; interestingly, ubiquitin is a center interacting molecule for several lipoxidized proteins

Figure 5: Overrepresented pathways and connections of genes encoding neuroketal-adducted proteins resulting from the analysis of enriched Gene Ontology (GO) terms using Cytoscape software, and including information from GO pathway and functions, KEEG, REACTOME and STRING databases.

Figure 6: Slot-blot quantification of soluble oligomers (antibody A11) (A) and total neuroketal (NKT) (B) levels in the parietal cortex, frontal cortex and cingulate gyrus in middle-aged and old-aged individuals; significant differences between age groups are analyzed with the Student's t test. Correlation of oligomers with age is found in the parietal and frontal cortices; correlations of NKT and age in the frontal cortex (C).

Figure 7: Significant positive correlations are found between soluble oligomers and neuroketal (NKT) levels in all regions (A). Relationships are summarized using principal component analysis (B).

List of figures:

Figure 1

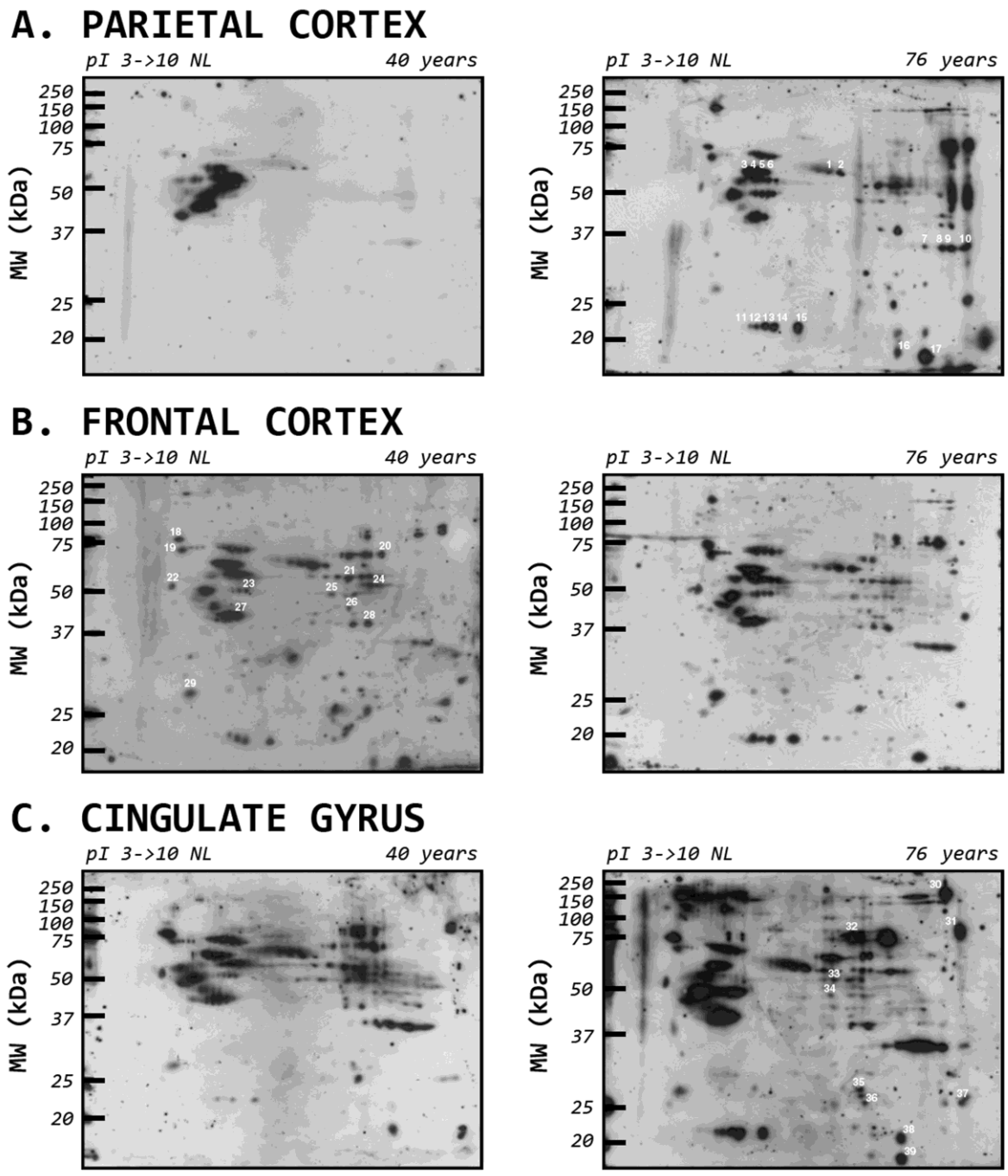

Figure 2

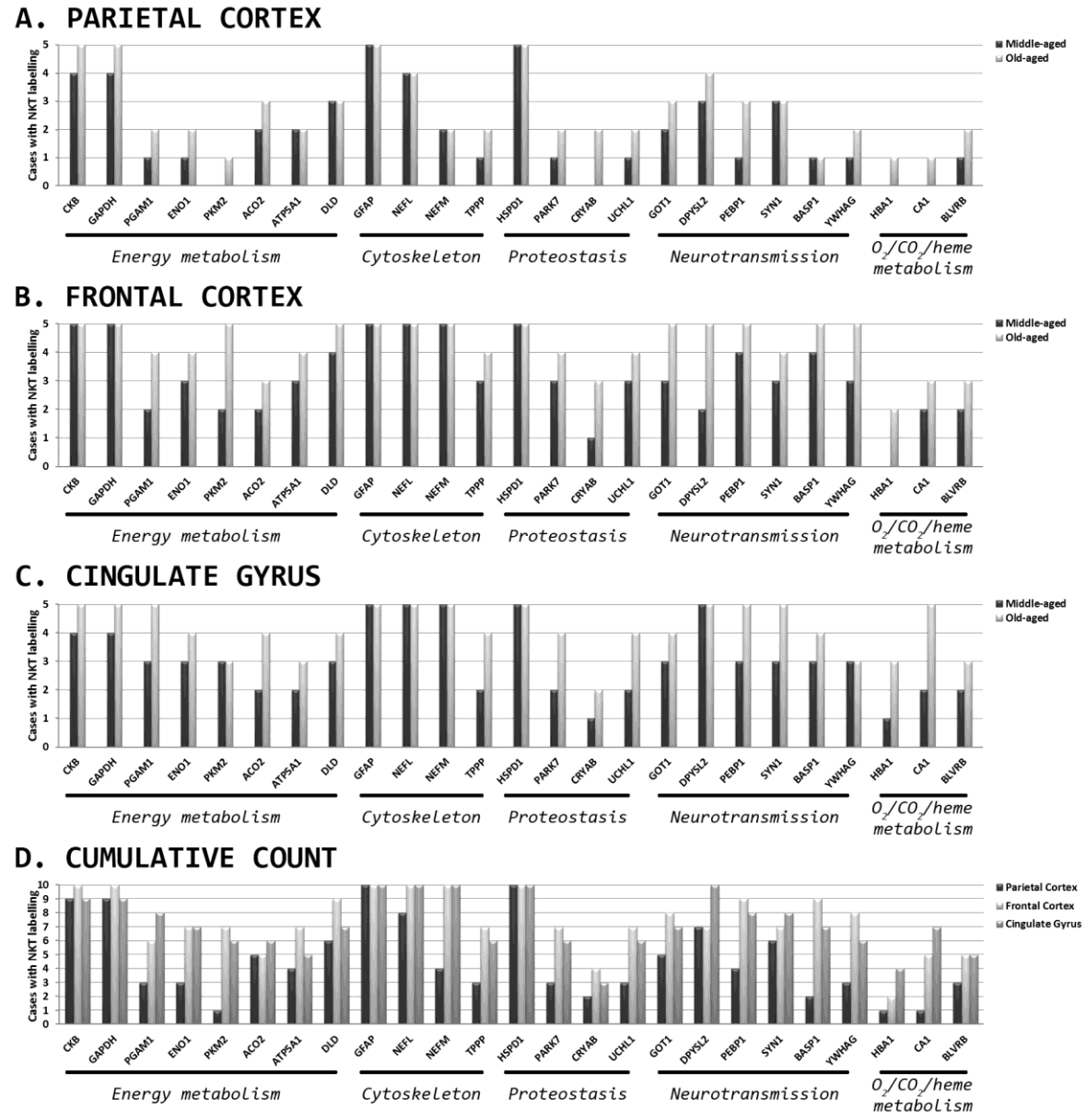

Figure 3

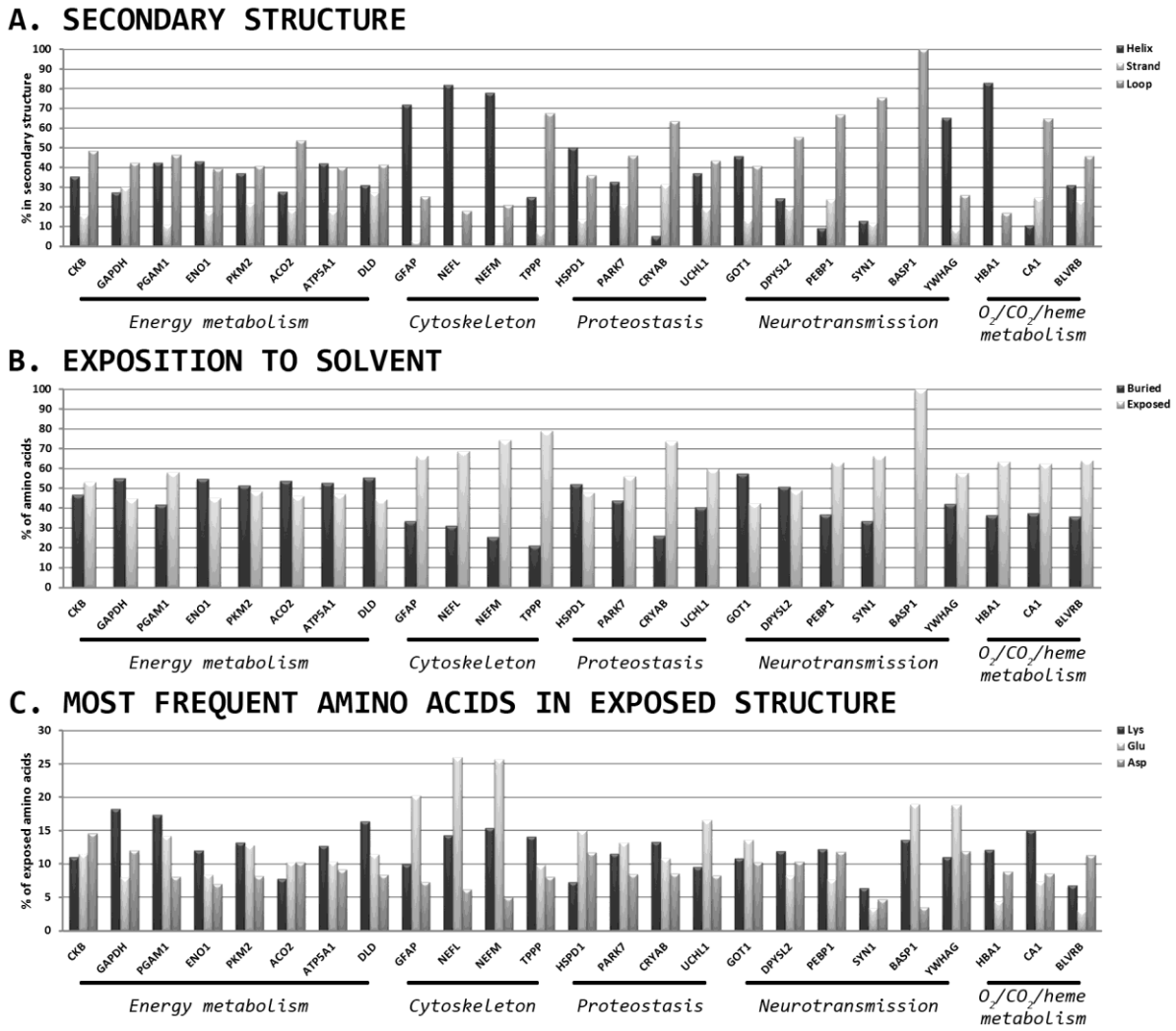

Figure 4

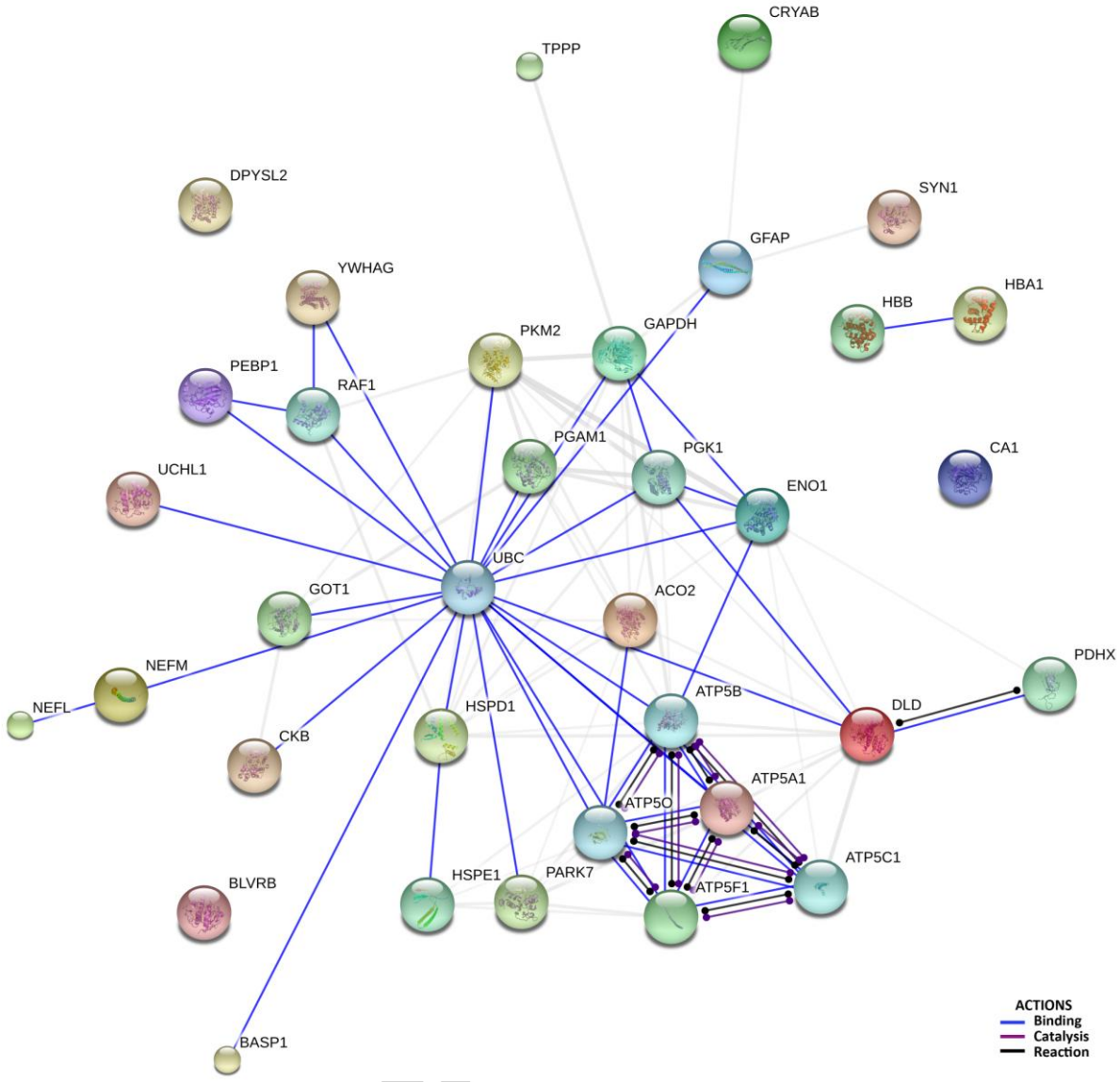

Figure 5

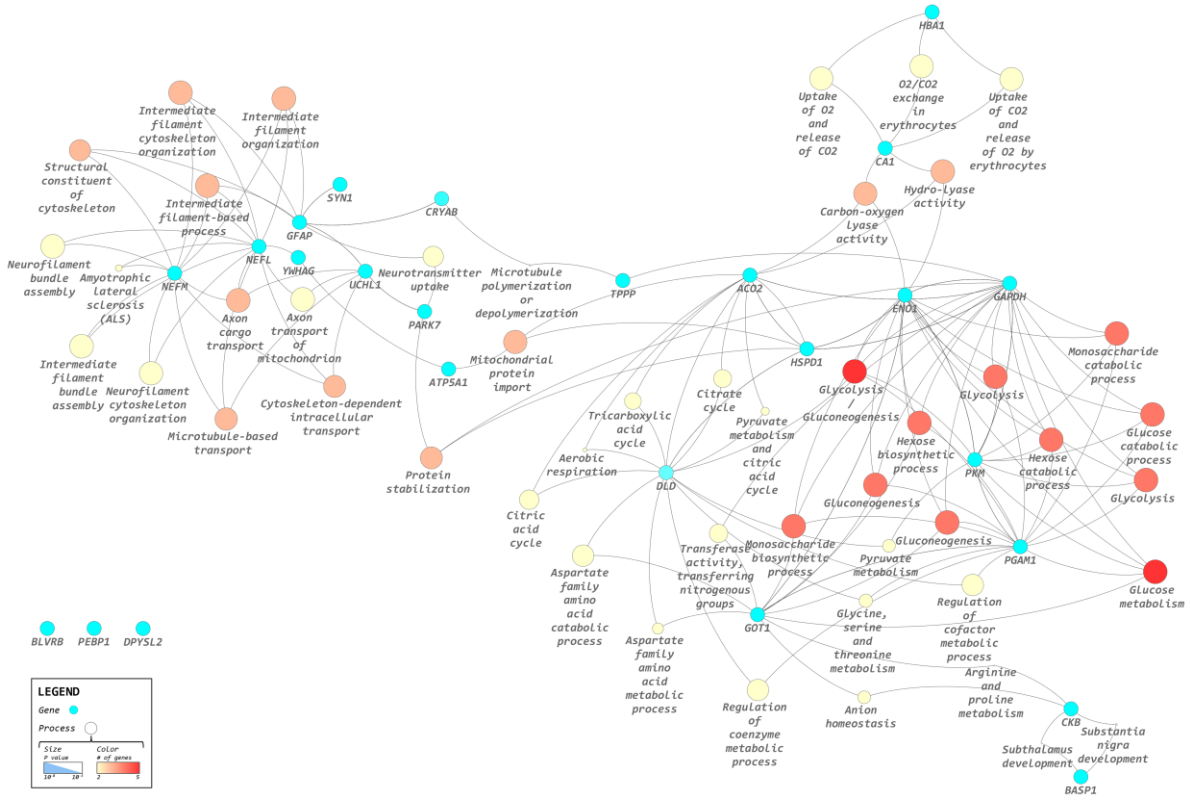

Figure 6

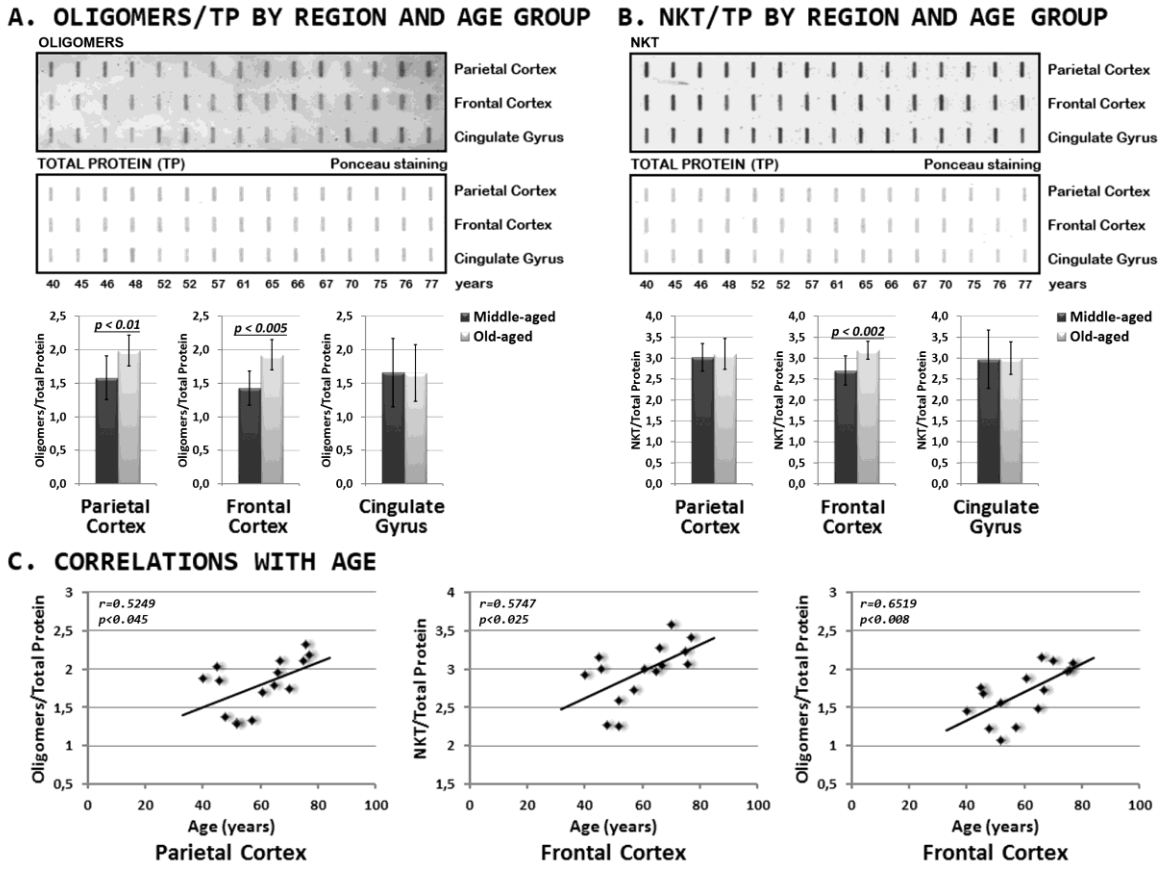

Figure 7

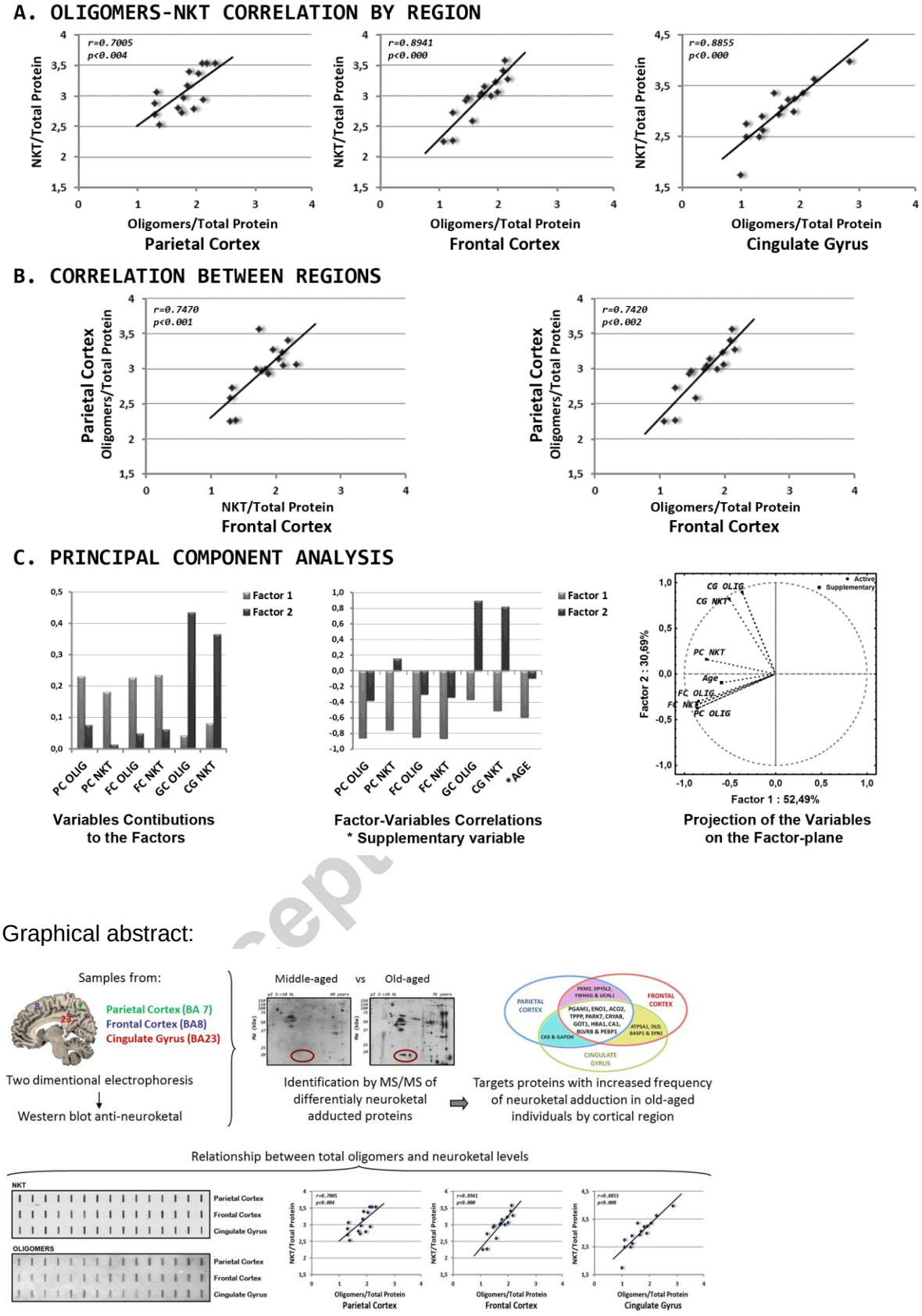

Graphical abstract:

Highlights

- Region-dependent brain protein lipoxidation occurs at middle age and increases in old age
- Proteins involved in energy metabolism, cytoskeleton, proteostasis, neurotransmission and O_2/CO_2, and heme metabolism are the main targets
- Sub-cellular localization, secondary structure and external exposition of certain amino acids are contributory factors in protein vulnerability
- Non-identified oligomers correlate with protein neuroketal adduction